Available online at www.CivileJournal.org

Civil Engineering Journal

(E-ISSN: 2476-3055; ISSN: 2676-6957)

Vol. 9, No. 11, November, 2023

Amending the Traditional 'ACI Commentary J_c Method' and Other Sources

Hugo Esquivel [1*], Guang Lin [2]

[1] *Department of Civil and Environmental Engineering, Universidad de la Costa, Barranquilla, Colombia.*

[2] *Department of Mathematics, School of Mechanical Engineering, Purdue University, West Lafayette, Indiana, United States.*

Received 21 June 2023; Revised 11 October 2023; Accepted 24 October 2023; Published 01 November 2023

Abstract

This article aims to amend the traditional formulas for polar moment of inertia suggested in Section R8.4.4.2.3 of ACI 318-19 and other sources. The authors claim that these formulas have been incorrectly derived as far back as 1960s due to an incorrect implementation of Steiner's theorem (parallel axis theorem) for sections spanning in three-dimensional space. To support the claim, a formal proof using elementary calculus is presented in order to obtain the correct formulas with mathematical rigor. Then, the implications of using the traditional formulas versus the correct ones are investigated with the solution of a design problem related to a combined footing.

Keywords: ACI 318-19; J_c Method; Slab-Column Connections; Structural Design; Two-Way Shear Action.

1. Introduction

The traditional 'ACI Commentary J_c Method,' presented nowadays in Section R8.4.4.2.3 of ACI 318-19 [1], has been extensively used in design and other sources [2-18] to check the maximum shear stresses developed around a slab-column connection due to the effect produced by an unbalanced moment at the slab-column connection. In this type of connections, the critical (shear) section is usually located at $d/2$ from the face of the column, as in Fig. 1 which depicts the critical section of an interior column with rectangular cross section c_1-by-c_2 and effective slab depth d. Because the actual distribution of shear stresses along the critical section is in most cases complex to determine, the ACI Code still permits the use of the theory of elasticity along with the further assumption that the 'connection's (horizontal) plane remains plane after deformation' to estimate the order of magnitude of such stresses (Section 8.4.4.2.3 of ACI 318-19). Hence, under the premise that shear stresses will remain essentially linear about the centroid of the critical section, the shear stress, v_y, developed at point P with coordinate x can readily be determined by:

$$v_y(x) = \frac{V_y}{b_0 d} + \frac{\gamma_v M_z x}{\bar{I}_z} \quad (1)$$

where V_y is the shear force acting on the critical section (positive if the force acts in the positive y-direction), b_0 is the perimeter of the critical section, d is the distance from the extreme compression fiber to the centroid of the longitudinal reinforcement on the tension side of the slab, γ_v is the fraction of unbalanced moment that is to be transferred by shear stresses on the critical section, M_z is the unbalanced moment acting on the slab-column connection (positive if the moment acts in the positive z-direction), $\gamma_v M_z$ is the torsional moment acting on the

* Corresponding author: hesquive@cuc.edu.co

http://dx.doi.org/10.28991/CEJ-2023-09-11-015

critical section, $\bar{I}_z$ is the (centroidal) polar moment of inertia of the critical section, and x is the location of point P with coordinate x where the shear stress, $v_y(x)$, is to be computed. Furthermore, Sections 8.4.4.2.2 and 8.4.2.2.2 of ACI 318-19 define the fraction γ_v as:

$$\gamma_v = 1 - \frac{1}{1+\frac{2}{3}\sqrt{\frac{b_1}{b_2}}} \tag{2}$$

where b_1 is the dimension of the critical section measured in the direction perpendicular to the torsional moment $\gamma_v M_z$, and b_2 is the dimension of the critical section perpendicular to b_1 (Figure 1). It is worth mentioning that if $v_y(x)$ is positive, the shear stress (at point P with coordinate x) acts in the positive y-direction, based on the adopted sign convention defined above.

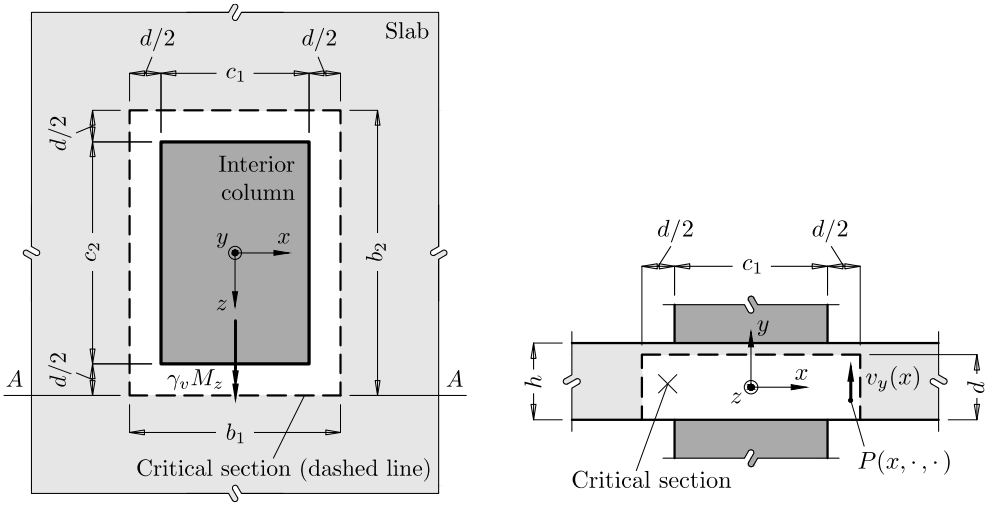

(a) Plan view **(b) Section AA**

Figure 1. A typical, interior slab-column connection

The polar moment of inertia, $\bar{I}_z$ (also referred to as J_c), of an interior slab-column connection has been historically presented in the ACI Code (e.g., as of ACI 318-63 [2]) as:

$$\bar{I}_z = 2\left[\tfrac{1}{12}b_1 d^3 + \tfrac{1}{12}d b_1^3\right] + 2\left[b_2 d\left(\tfrac{1}{2}b_1\right)^2\right]. \tag{3}$$

However, this expression, first suggested by Di Stasio and Van Buren in 1960 [8], is not entirely correct since it does not consider the fact that the two side faces parallel to $\gamma_v M_z$ have a definite height equal to d, which also contributes to the total polar moment of inertia of the critical section. To account for this extra contribution, the formula for $\bar{I}_z$ should rather be written as:

$$\bar{I}_z = 2\left[\tfrac{1}{12}b_1 d^3 + \tfrac{1}{12}d b_1^3\right] + 2\left[\tfrac{1}{12}b_2 d^3 + b_2 d\left(\tfrac{1}{2}b_1\right)^2\right], \tag{4}$$

where the missing term in Equation 3 is:

$$2\left[\tfrac{1}{12}b_2 d^3\right].$$

Although Section R8.4.4.2.3 of ACI 318-19 [1] does point out that J_c is a property 'analogous' to polar moment of inertia, none of the sources consulted [1-18] discusses the reason why the missing term can be neglected. For instance, Wight & MacGregor [17] tacitly states that the polar moment of inertia, $\bar{I}_z$, of critical sections spanning in three-dimensional space is ill-defined and that one way to consider the contribution of the side faces (i.e., those faces parallel to $\gamma_v M_z$) is to reduce their geometry as points with area—an unnecessary simplification to make, nonetheless, as we will see later. In this case, the missing term is a consequence of the simplification. Moreover, neglecting the missing term does not make the formula any nicer or simpler to use but it does cause the formula to lose a certain amount of information when dealing with deep slab-column connections.

In the following section, a formal proof of Equation 4 is provided to demonstrate the correctness of authors' claim using elementary calculus. This is followed by the proofs of the J_c expressions required for an edge and a corner slab-column connection. The article ends with a practical example to investigate the numerical differences between the traditional and the correct J_c expressions in the solution of a design problem related to a combined footing.

2. Proof

2.1. Definition of Polar Moment of Inertia

In mechanics, the polar moment of inertia of a section about the z-axis is defined by.

$$I_z = \int_A r^2(x,y)\,\mathrm{d}A, \tag{5}$$

where $\mathrm{d}A$ is the differential element of total area A, and r is the (shortest) distance measured from the z-axis to $\mathrm{d}A$. The quantity r^2 is already given as a function of x and y because a set of Cartesian coordinate systems will be used in the following sections.

2.2. Proof for an Interior Slab-column Connection

The critical section of an interior slab-column connection is usually comprised by four mutually orthogonal faces, as in Figure 2-a. The centroid, C, of such a section is located at $b_1/2$ from face 2, at $b_2/2$ from face 1, and at $d/2$ from the bottom of the critical section. For convenience, a (standard) Cartesian coordinate system is defined at point C, such that: (1) the z-axis is oriented parallel to the torsional moment $\gamma_v M_z$, and (2) the plane generated by the x and z axes is parallel to the slab's plane. As observed, the quantities r^2 and $\mathrm{d}A$ for faces 1 and 3 are given by:

$$r_1^2(x,y) = r_3^2(x,y) = x^2 + y^2 \tag{6}$$

$$\mathrm{d}A_1 = \mathrm{d}A_3 = \mathrm{d}x\mathrm{d}y \tag{7}$$

and for faces 2 and 4 they are given by:

$$r_2^2(x,y) = r_4^2(x,y) = \left(\tfrac{1}{2}b_1\right)^2 + y^2 \tag{8}$$

$$\mathrm{d}A_2 = \mathrm{d}A_4 = \mathrm{d}z\mathrm{d}y. \tag{9}$$

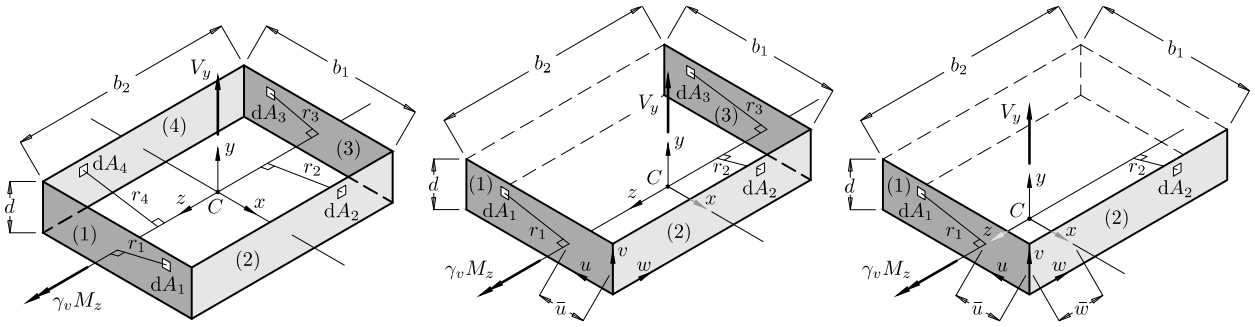

(a) Interior slab-column connection (b) Edge slab-column connection (c) Corner slab-column connection

Figure 2. Critical sections for different types of slab-column connections

Substituting these quantities into Equation 5 yields the $\bar{I}_z$ of an interior slab-column connection:

$$\bar{I}_z = \int_A r^2(x,y)\,\mathrm{d}A = 2\int_{A_1} r_1^2(x,y)\,\mathrm{d}A_1 + 2\int_{A_2} r_2^2(x,y)\,\mathrm{d}A_2 = 2\int_{-\frac{d}{2}}^{\frac{d}{2}}\int_{-\frac{b_1}{2}}^{\frac{b_1}{2}}(x^2+y^2)\,\mathrm{d}x\mathrm{d}y + 2\int_{-\frac{d}{2}}^{\frac{d}{2}}\int_{-\frac{b_2}{2}}^{\frac{b_2}{2}}\left[\left(\tfrac{1}{2}b_1\right)^2 + y^2\right]\mathrm{d}z\mathrm{d}y = 2\left[\tfrac{1}{12}b_1 d^3 + \tfrac{1}{12}d b_1^3\right] + 2\left[\tfrac{1}{12}b_2 d^3 + b_2 d\left(\tfrac{1}{2}b_1\right)^2\right]. \tag{10}$$

This result should not be surprising. The first summand is the usual $\bar{I}_z$ for faces 1 and 3; i.e., the sum of the moments of inertia about the x and y axes for faces 1 and 3. The second summand is nothing but the result of implementing Steiner's theorem on faces 2 and 4.

2.3. Proof for an Edge Slab-column Connection

Let's now consider the edge slab-column connection depicted in Figure 2-b. The centroid, C, of the critical section is located at $\bar{u}$ from face 2, at $b_2/2$ from face 1, and at $d/2$ from the bottom of the critical section, where:

$$\bar{u} = \frac{1}{A}\int_A u\,\mathrm{d}A = \frac{1}{2A_1+A_2}\left(2\int_{A_1} u\,\mathrm{d}A_1 + \int_{A_2} 0\,\mathrm{d}A_2\right) = \frac{2}{2b_1 d + b_2 d}\int_0^d\int_0^{b_1} u\,\mathrm{d}u\mathrm{d}v = \frac{b_1^2}{2b_1+b_2} = \frac{b_1^2}{b_0}, \tag{11}$$

after noticing that $A_1 = A_3 = b_1 d$, $A_2 = b_2 d$, $\mathrm{d}A_1 = \mathrm{d}A_3 = \mathrm{d}u\mathrm{d}v$, $\mathrm{d}A_2 = \mathrm{d}v\mathrm{d}w$, and $b_0 = 2b_1 + b_2$.

A Cartesian coordinate system is once again defined at point C using the same orientation as before. This time, the quantities r^2 and $\mathrm{d}A$ for faces 1, 2 and 3 are given by:

$$r_1^2(x,y) = r_3^2(x,y) = x^2 + y^2 \tag{12}$$

$$r_2^2(x,y) = \bar{u}^2 + y^2 \tag{13}$$

$$\mathrm{d}A_1 = \mathrm{d}A_3 = \mathrm{d}x\mathrm{d}y \tag{14}$$

$$\mathrm{d}A_2 = \mathrm{d}z\mathrm{d}y. \tag{15}$$

Hence, the $\bar{I}_z$ of an edge slab-column connection is:

$$\bar{I}_z = \int_A r^2(x,y)\,\mathrm{d}A = 2\int_{A_1} r_1^2(x,y)\,\mathrm{d}A_1 + \int_{A_2} r_2^2(x,y)\,\mathrm{d}A_2 = 2\int_{-\frac{d}{2}}^{\frac{d}{2}}\int_{-(b_1-\bar{u})}^{\bar{u}}(x^2+y^2)\,\mathrm{d}x\mathrm{d}y + \int_{-\frac{d}{2}}^{\frac{d}{2}}\int_{-\frac{b_2}{2}}^{\frac{b_2}{2}}(\bar{u}^2+y^2)\,\mathrm{d}z\mathrm{d}y = 2\left[\tfrac{1}{12}b_1d^3 + \tfrac{1}{12}db_1^3 + b_1d\left(\tfrac{1}{2}b_1-\bar{u}\right)^2\right] + \left[\tfrac{1}{12}b_2d^3 + b_2d\bar{u}^2\right] \tag{16}$$

Again, both these summands are the result of implementing Steiner's theorem on each face.

2.4. Proof for a Corner Slab-column Connection

Lastly, let's consider the corner slab-column connection depicted in Figure 2-c. The centroid, C, of the critical section is located at $\bar{u}$ from face 2, at $\bar{w}$ from face 1, and at $d/2$ from the bottom of the critical section, where:

$$\bar{u} = \frac{1}{A}\int_A u\,\mathrm{d}A = \frac{1}{A_1+A_2}\left(\int_{A_1} u\,\mathrm{d}A_1 + \int_{A_2} 0\,\mathrm{d}A_2\right) = \frac{1}{b_1d+b_2d}\int_0^d\int_0^{b_1} u\,\mathrm{d}u\mathrm{d}v = \frac{b_1^2}{2(b_1+b_2)} = \frac{b_1^2}{2b_0} \tag{17}$$

and similarly,

$$\bar{w} = \frac{1}{A}\int_A v\,\mathrm{d}A = \frac{b_2^2}{2(b_1+b_2)} = \frac{b_2^2}{2b_0}, \tag{18}$$

whence $A_1 = b_1d$, $A_2 = b_2d$, $\mathrm{d}A_1 = \mathrm{d}u\mathrm{d}v$, $\mathrm{d}A_2 = \mathrm{d}v\mathrm{d}w$, and $b_0 = b_1 + b_2$.

The quantities r^2 and $\mathrm{d}A$ for faces 1 and 2 are given by:

$$r_1^2(x,y) = x^2 + y^2 \tag{19}$$

$$r_2^2(x,y) = \bar{u}^2 + y^2 \tag{20}$$

$$\mathrm{d}A_1 = \mathrm{d}x\mathrm{d}y \tag{21}$$

$$\mathrm{d}A_2 = \mathrm{d}z\mathrm{d}y \tag{22}$$

Hence, the $\bar{I}_z$ of a corner slab-column connection is:

$$\bar{I}_z = \int_A r^2(x,y)\,\mathrm{d}A = \int_{A_1} r_1^2(x,y)\,\mathrm{d}A_1 + \int_{A_2} r_2^2(x,y)\,\mathrm{d}A_2 = \int_{-\frac{d}{2}}^{\frac{d}{2}}\int_{-(b_1-\bar{u})}^{\bar{u}}(x^2+y^2)\,\mathrm{d}x\mathrm{d}y + \int_{-\frac{d}{2}}^{\frac{d}{2}}\int_{-\frac{b_2}{2}}^{\frac{b_2}{2}}(\bar{u}^2+y^2)\,\mathrm{d}z\mathrm{d}y = \left[\tfrac{1}{12}b_1d^3 + \tfrac{1}{12}db_1^3 + b_1d\left(\tfrac{1}{2}b_1-\bar{u}\right)^2\right] + \left[\tfrac{1}{12}b_2d^3 + b_2d\bar{u}^2\right] \tag{23}$$

As before, this same result could have been inferred from Steiner's theorem applied on faces 1 and 2.

3. Example

The following example is taken from Wight & MacGregor [17] on reinforced concrete (Example 15-5, p. 845) to provide context of the situation discussed here. The example (Figure 3) considers a combined footing supporting a 16-in-by-24-in exterior column ($c_1 = 16$ in and $c_2 = 24$ in), and a 24-in-square interior column. The height of the footing is 36 in, giving an effective depth of approximately $d = 32.5$ in. The shear force and unbalanced moment acting on the critical section of the exterior column are $V_y = 405$ kips and $M_z = -6{,}950$ kips-in, following the notation and sign convention adopted in this work.

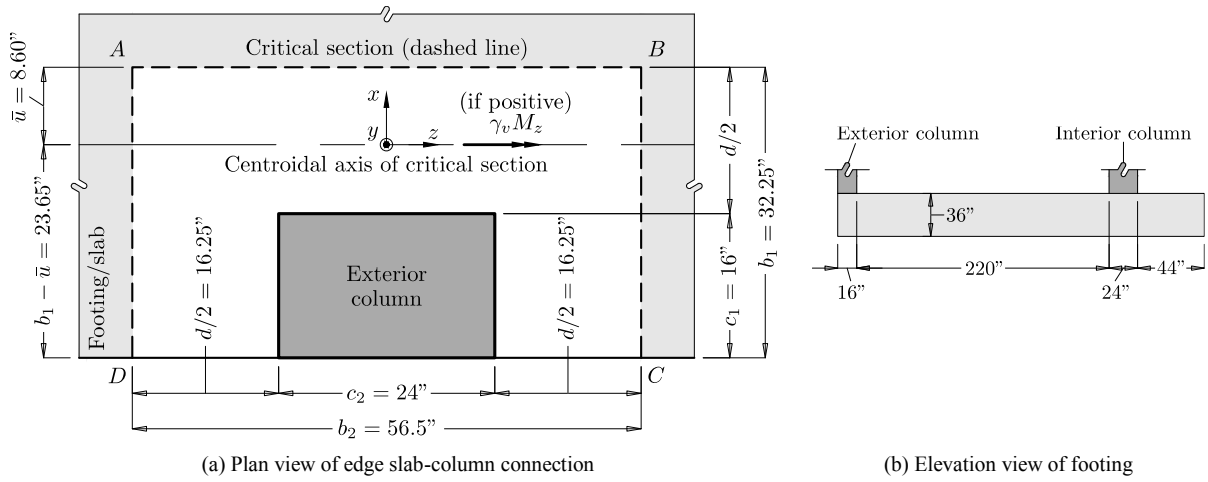

(a) Plan view of edge slab-column connection (b) Elevation view of footing

Figure 3. Combined footing (design problem taken from Example 15-5 of Wight & MacGregor [17])

The size of the critical section is characterized by the orthogonal dimensions b_1 and b_2, where:

$$b_1 = c_1 + \tfrac{1}{2}d = 16 + \tfrac{1}{2}(32.5) = 32.25 \text{ in} \tag{24}$$

$$b_2 = c_2 + d = 24 + 32.5 = 56.5 \text{ in.} \tag{25}$$

Therefore, the fraction of moment transferred by twist (Equation 2) is:

$$\gamma_v = 1 - \frac{1}{1+\frac{2}{3}\sqrt{\frac{b_1}{b_2}}} = 1 - \frac{1}{1+\frac{2}{3}\sqrt{\frac{32.25}{56.5}}} = 0.335, \tag{26}$$

and the perimeter of the critical section is:

$$b_0 = 2b_1 + b_2 = 2(32.25) + 56.5 = 121 \text{ in.} \tag{27}$$

According to Equation 11, the location of the (shear) centroid measured from face AB is:

$$\bar{u} = \frac{b_1^2}{b_0} = \frac{(32.25)^2}{121} = 8.60 \text{ in} \tag{28}$$

Then, following the historical approach, Wight and MacGregor [17] computes the polar moment of inertia of the critical section using:

$$J_c = 2\left[\tfrac{1}{12}b_1 d^3 + \tfrac{1}{12}db_1^3 + b_1 d\left(\tfrac{1}{2}b_1 - \bar{u}\right)^2\right] + b_2 d\bar{u}^2 = 2\left[\tfrac{1}{12}(32.25)(32.5)^3 + \tfrac{1}{12}(32.5)(32.25)^3 + (32.25)(32.5)\left(\tfrac{1}{2}(32.25) - 8.60\right)^2\right] + (56.5)(32.5)(8.60)^2 = 621{,}000 \text{ in}^4. \tag{29}$$

However, using the correct expression for J_c (Equation 16) produces

$$J_c = 2\left[\tfrac{1}{12}b_1 d^3 + \tfrac{1}{12}db_1^3 + b_1 d\left(\tfrac{1}{2}b_1 - \bar{u}\right)^2\right] + \left[\tfrac{1}{12}b_2 d^3 + b_2 d\bar{u}^2\right] = 2\left[\tfrac{1}{12}(32.25)(32.5)^3 + \tfrac{1}{12}(32.5)(32.25)^3 + (32.25)(32.5)\left(\tfrac{1}{2}(32.25) - 8.60\right)^2\right] + \left[\tfrac{1}{12}(56.5)(32.5)^3 + (56.5)(32.5)(8.60)^2\right] = 782{,}000 \text{ in}^4, \tag{30}$$

which turns out to be about 25% greater than the one calculated previously.

Moreover, the shear stress, v_y, developed at a point P with coordinate x is determined with Equation 1:

$$v_y(x) = \frac{V_y}{b_0 d} + \frac{\gamma_v M_z x}{J_c} = \frac{405}{(121)(32.5)} + \frac{(0.335)(-6{,}950)x}{782{,}000} = 0.103 - 0.00298x \text{ (in ksi, and } x \text{ in inches).} \tag{31}$$

From this it can be shown that the maximum shear stress is produced at

$$x = -(b_1 - \bar{u}) = -(32.25 - 8.60) = -23.65 \text{ in,} \tag{32}$$

and that its value is equal to 0.173 ksi. However, if the traditional expression for J_c were to be employed, a maximum shear stress of 0.192 ksi would have been obtained, producing an overestimation of 10%. Though this overestimation would have not been a concern in this case, there are indeed situations in which it can lead to undesirable conservative designs, as is the case with deeper slabs or mat foundations where d is sufficiently large.

Other implications of having a large d are demonstrated below.

Observe that when d is sufficiently large, b_1, b_2, b_0 and $\bar{u}$ approach asymptotically to the following expressions: $b_1 \sim \frac{1}{2}d, b_2 \sim d, b_0 \sim 2d, \bar{u} \sim \frac{1}{8}d$.

Inserting these expressions into Equations 29 and 30 give, respectively, the asymptotic behavior for each J_c. Namely,

$$J_c \sim \frac{13}{96}d^4 \text{ for the traditional expression, and } J_c \sim \frac{7}{32}d^4 \text{ for the correct expression.} \quad (33)$$

Ergo, as d tends to infinity, the ratio $J_{c,\text{ correct}}/J_{c,\text{ traditional}}$ tends to $\frac{21}{13} \approx 1.62$, which means that numerical differences of up to 62% can be expected between both expressions. Furthermore, if V_y were sufficiently small compared to the effect produced by $\gamma_v M_z$, the ratio $v_{y,\text{ correct}}/v_{y,\text{ traditional}}$ would tend to $\frac{13}{21} \approx 0.62$ as d tends to infinity. Hence, a design based on the traditional J_c expression can produce an overestimation of up to 62% in the worst-case load scenario. This is equivalent to adding an unwanted safety factor of 1.62 to the design of the slab-column connection.

Finally, it is observed that as d tends to zero, the ratio $J_{c,\text{ correct}}/J_{c,\text{ traditional}}$ tends to 1. This is why in shallow slab-column connections where d is sufficiently small (e.g., as in flat floor systems), no significant numerical differences are expected between $J_{c,\text{ traditional}}$ and $J_{c,\text{ correct}}$. In those cases, both expressions produce the same order of magnitude.

4. Conclusions

This article has presented the correct formulas for polar moment of inertia needed in Section R8.4.4.2.3 of ACI 318-19 [1] and other sources (e.g., [2-18]). The formulas were derived for three different types of slab-column connections to show how to treat each case individually. For other types, a similar approach can be followed. The implications of using the traditional formula versus the correct formula in the design of an edge slab-column connection were presented in Section 3, from where it was shown that numerical differences of up to 62% can be expected if the slab-column connection is sufficiently thick.

The purpose of this article was twofold. First, to realize that Section R8.4.4.2.3 of ACI 318-19 needs to be amended so that the second paragraph of the commentary reads:

"For an interior column, J_c may be calculated by:

$J_c =$ centroidal polar moment of inertia of assumed critical section,

$$= \frac{d(c_1+d)^3}{6} + \frac{(c_1+d)d^3}{6} + \frac{(c_2+d)d^3}{6} + \frac{d(c_2+d)(c_1+d)^2}{2}."$$

(This expression is equivalent to Equation 10 with $b_1 = c_1 + d$ and $b_2 = c_2 + d$.)

Second, to hope that other authors will eventually take note and adopt the correct J_c expressions for use in their new manuscript releases. The authors believe that using the correct expressions for J_c would lead to a more consistent implementation of the traditional 'ACI Commentary Jc Method' in the years to come, especially for deep slab-column connections resisting significant unbalanced moment.

It is now up to the research community to establish whether the proposed amendment to the Jc method produces a safe procedure to design deep slab-column connections as per ACI 318. It is suggested that more research is devoted to this topic in order to obtain more reliable designs in the future.

As a final remark, one may wonder why the ACI Code defines J_c as a property *analogous* to polar moment of inertia. One plausible reason for resorting to the analogy is that it is customary to think that the concept of polar moment of inertia is limited to sections that can be laid out on a flat sheet of paper. In mechanics, however, this concept is more general and can encompass three-dimensional space as well. The more accurate definition of J_c was given in Section 2.1.

5. Declarations

5.1. Author Contributions

Conceptualization, H.E.; methodology, H.E.; validation, H.E.; formal analysis, H.E.; investigation, H.E.; resources, H.E.; data curation, H.E.; writing—original draft preparation, H.E.; writing—review and editing, H.E. and G.L.; visualization, H.E.; supervision, H.E. and G.L.; project administration, H.E. and G.L. All authors have read and agreed to the published version of the manuscript.

5.2. Data Availability Statement

The data presented in this study are available in the article.

5.3. Funding

The authors received no financial support for the research, authorship, and/or publication of this article.

5.4. Conflicts of Interest

The authors declare no conflict of interest.

6. References

[1] ACI Committee 318-19. (2019). Building code requirements for structural concrete (ACI 318-19) and commentary (ACI 318R-19). American Concrete Institute (ACI), Michigan, United States. doi:10.14359/51716937.

[2] ACI Committee 318-63. (1963). Building code requirements for structural concrete (ACI 318-63). American Concrete Institute (ACI), Michigan, United States.

[3] ACI. (2021). The Reinforced Concrete Design Handbook A Companion to ACI 318-19. American Concrete Institute (ACI), Michigan, United States.

[4] Collins, M. P., & Mitchell, D. (1997). Prestressed concrete structures. Response Publications, Ontario, Canada.

[5] CIS. (2022). Reinforced concrete slab design manual for ETABS (Version 20). Computers & Structures, California, United States.

[6] Clarke, L. A., & Cope, R. J. (1984). Concrete slabs: analysis and design. CRC Press, London, United Kingdom. doi:10.1201/9781482292794.

[7] Darwin, D., & Dolan, C. W. (2021). Design of concrete structures (16th Ed.). McGraw-Hill Education, New York, United States.

[8] Stasio, J., & Buren, M. P. (1960). Transfer of Bending Moment Between Flat Plate Floor and Column. ACI Journal Proceedings, 57(9), 299–314. doi:10.14359/8022.

[9] Dolan, C. W., & Hamilton, H. R. (2019). Prestressed Concrete: building, design, and construction. Springer, Cham. Switzerland. doi:10.1007/978-3-319-97882-6.

[10] Islam, S. (1973). Limit design of reinforced concrete slabs: openings and slab-column connections. Ph.D. Thesis, University of Canterbury, Christchurch, New Zealand.

[11] Lin, T. Y., & Burns, N. H. (1981). Design of prestressed concrete structures. (3rd Ed.). John Wiley & Sons, Hoboken, United States.

[12] McCormac, J. C., & Brown, R. H. (2015). Design of reinforced concrete. (10th Ed.). John Wiley & Sons, Hoboken, United States.

[13] Naaman, A. E. (2004). Prestressed concrete analysis and design: fundamentals. (2nd Ed.). Techno Press, Michigan, United States.

[14] Nawy, E. G. (2009). Prestressed concrete: a fundamental approach (5nd Ed.). Pearson Education, New Jersey, United States.

[15] Park, R., & Gamble, W. L. (1999). Reinforced concrete slabs. (2nd Ed.). John Wiley & Sons, Hoboken, United States.

[16] PTI. (2006). Post-Tensioning Manual (6th Ed.). Post-Tensioning Institute, Arizona, United States.

[17] Wight, J. K., & MacGregor, J.G. (2012). Reinforced concrete: mechanics and design (6th Ed.). Pearson Education, New Jersey, United States.

[18] Zhou, Y. (2019). Seismic Performance Assessment and Nonlinear Modeling Parameters for Slab-Column Connections. Ph.D. Thesis, College Station, United States.